Path integrals for Fokker–Planck dynamics with singular diffusion: accurate factorization for the time evolution operator

Alexander N. Drozdov, Peter Talkner

Angaben zur Veröffentlichung / Publication details:

Drozdov, Alexander N., and Peter Talkner. 1998. "Path integrals for Fokker–Planck dynamics with singular diffusion: accurate factorization for the time evolution operator." *The Journal of Chemical Physics* 109 (6): 2080–91. https://doi.org/10.1063/1.476721.

Path integrals for Fokker–Planck dynamics with singular diffusion: Accurate factorization for the time evolution operator

Cite as: J. Chem. Phys. **109**, 2080 (1998); https://doi.org/10.1063/1.476721
Submitted: 27 January 1998 • Accepted: 04 May 1998 • Published Online: 30 September 1998

Alexander N. Drozdov and Peter Talkner

Path integrals for Fokker–Planck dynamics with singular diffusion: Accurate factorization for the time evolution operator

Alexander N. Drozdov[a] and Peter Talkner
General Energy Research, Paul Scherrer Institute, CH-5232 Villigen, Switzerland

(Received 27 January 1998; accepted 4 May 1998)

Fokker–Planck processes with a singular diffusion matrix are quite frequently met in Physics and Chemistry. For a long time the resulting noninvertability of the diffusion matrix has been looked as a serious obstacle for treating these Fokker–Planck equations by various powerful numerical methods of quantum and statistical mechanics. In this paper, a path-integral method is presented that takes advantage of the singularity of the diffusion matrix and allows one to solve such problems in a simple and economic way. The basic idea is to split the Fokker–Planck equation into one of a linear system and an anharmonic correction and then to employ a symmetric decomposition of the short time propagator, which is exact up to a high order in the time step. Just because of the singularity of the diffusion matrix, the factors of the resulting product formula consist of well behaved propagators. In this way one obtains a highly accurate propagation scheme, which is simultaneously fast, stable, and computationally simple. Because it allows much larger time steps, it is more efficient than the standard propagation scheme based on the Trotter splitting formula. The proposed method is tested for Brownian motion in different types of potentials. For a harmonic potential we compare to the known analytic results. For a symmetric double well potential we determine the transition rates between the two wells for different friction strengths and compare them with the crossover theories of Mel'nikov and Meshkov and Pollak, Grabert, and Hänggi. Using a properly defined energy loss of the deterministic particle dynamics, we obtain excellent agreement. The methodology is outlined for a large class of processes defined by generalized Langevin equations and processes driven by colored noise. © *1998 American Institute of Physics.* [S0021-9606(98)01230-6]

I. INTRODUCTION

The classical motion of a Brownian particle in phase space, under the influence of a potential $U(x)$, is an important physical process which plays a central role in many practical dynamical problems.[1–5] It is described by two coupled Langevin equations that in mass-weighted variables read

$$\dot{x}=v,\quad \dot{v}=-\gamma v-U'(x)+f(t). \tag{1.1}$$

Here the dot denotes the time derivative, and the prime the derivative with respect to the coordinate. The medium influences the particle by a velocity-proportional damping force $-\gamma v$ and a Gaussian white random force $f(t)$ normalized to

$$\langle f(t)\rangle=0,\ \langle f(t)f(s)\rangle=2\gamma D\,\delta(t-s), \tag{1.2}$$

where γ is the friction coefficient and D a measure of the noise strength. For a thermal bath it is proportional to the bath temperature, $D=k_BT$. When positions are measured in multiples of a characteristic length l of the potential and time in thermal units $t_{\rm th}=l/\sqrt{k_BT}$ the diffusion constant D becomes unity. The potential then becomes $U(x)=\tilde{U}(\tilde{x}/l)/(k_BT)$ and the damping constant $\gamma=\tilde{\gamma}l/\sqrt{k_BT}$, where the tilde denotes the respective quantities in dimensional units.

An equivalent description can be given in terms of a two-dimensional Fokker–Planck equation, which governs the time evolution of the probability density of finding the particle at time t at the phase space point x, v,

$$\begin{aligned}\partial_t P(x,v,t)&=LP(x,v,t)\\&=[-v\,\partial_x+U'(x)\partial_v+\gamma\partial_v(v+D\partial_v)]P(x,v,t),\end{aligned} \tag{1.3}$$

with L being the Fokker–Planck operator. Having only a vv-component, it is obvious that the diffusion matrix of Eq. (1.3), i.e., the coefficient matrix of second derivatives with respect to position and velocity, does not possess an inverse. Due to detailed balance the stationary solution of the Fokker–Planck operator is given by the Maxwell–Boltzmann distribution

$$P_s(x,v)=Z^{-1}\exp\{-[\tfrac{1}{2}v^2+U(x)]/D\}, \tag{1.4}$$

with a partition function Z.

The above model, although simple, is of enormous utility in understanding and evaluating the influence of a medium on dynamical processes. It is commonly used in studies of superionic conductors, Josephson tunneling junctions, nonlinear optics, nucleation, and escape rate theories.[1] The escape of a Brownian particle is but one phenomenon that can be described by this model.[2] The model has been extended in various directions in order to cover more general

[a]Present address: Física Teórica, Universidad de Sevilla, Apartado de Correos 1065, Sevilla 41080, Spain. Permanent address: Institute for High Temperatures, 13/19 Izhorskaya Street, 127412 Moscow, Russia.

environments that cause random forces with finite correlation times. For equilibrium systems generalized Langevin equations have been introduced.[6] They are characterized by a finite correlation function of the random force and a memory kernel, i.e., by a retarded, instead of the instantaneous, friction force of an ordinary Langevin equation. This memory kernel is directly related to the correlation function of the random force by a fluctuation-dissipation theorem. Nonequilibrium systems are frequently modeled by colored noise but instantaneous friction.[7,8] Except for linear systems, only few analytic methods exist to treat the resulting non-Markovian processes. Various effective Markovian approximations have been proposed for such non-Markovian processes. But all of them are valid only in particular limiting cases.[8–11] As however, the non-Markovian character may strongly influence the dynamics, reliable methods are needed. A straightforward way of dealing with a non-Markovian process is to add a sufficient number of supplementary variables such that the resulting process is Markovian in the enlarged phase space.[12,13] Although the particular forms of the resulting Markovian Langevin and Fokker–Planck equations depend on the noise correlation function, they nevertheless have one common feature, namely, that their diffusion matrices are singular. The latter property makes it impossible to use powerful variational methods of quantum mechanics and also is an obstacle for employing an efficient power series expansion technique.[14] We shall here show that just this property allows one to construct a highly accurate path integral representation of the time evolution of these processes.

Since it is generally not possible to obtain closed form analytic solutions of second-order partial differential equations, a number of numerical methods have been devised to integrate Brownian motion on a grid, such as finite-difference schemes,[15] basis set expansions,[5,16,17] computer simulations,[18] and path integral techniques.[19–23] However, these methods suffer from various different shortcomings. Standard methods such as basis set expansions and finite-difference schemes can, in principle, provide very accurate results with intensive computation efforts. Their utility, however, is strongly limited by the storage requirements and execution time that both grow exponentially with the number of coupled degrees of freedom. For a finite-difference representation, the requirement of numerical stability severely restricts the permitted time step. This is also true for computer simulations of Langevin dynamics, which are less restrictive with respect to the dimensionality than the above mentioned methods. A disadvantage of computer simulation techniques is that they suffer from statistical errors. In contrast, the path integral formulation of the Fokker-Planck equation provides a numerically stable solution which is free of statistical errors and requires a computational effort that increases only slowly with the dimensionality of the system. Its efficacy, however, depends crucially on the accuracy of the short time propagator used.

In practice, numerical evaluation of a path integral reduces to the calculation of a multidimensional integral reading

$$P(\mathbf{q},t)=\int\prod_{n=0}^{N-1}d\mathbf{q}^n P_k(\mathbf{q}^{n+1},\Delta t|\mathbf{q}^n)P(\mathbf{q}^0,0)+O(t^{k+1}/N^k), \tag{1.5}$$

with $\Delta t=t/N$ and $\mathbf{q}^N=\mathbf{q}\equiv(q_1,\ldots,q_m)$. Here k denotes the order of approximation taken for the single step propagator

$$P(\mathbf{q},\Delta t|\mathbf{q}^0)\equiv\langle\mathbf{q}|e^{\Delta tL}|\mathbf{q}^0\rangle=P_k(\mathbf{q},\Delta t|\mathbf{q}^0)+O(\Delta t^{k+1}). \tag{1.6}$$

It is clear that the number N of time steps can be reduced if the accuracy of the short time propagator P_k can be extended to longer time intervals Δt. The most common procedure of approximating the short time propagator utilizes the Trotter splitting formula

$$e^{\Delta t(A+B)}=S_2(\Delta t)+O(\Delta t^3),\qquad S_2(\Delta t)=e^{\Delta tA/2}e^{\Delta tB}e^{\Delta tA/2}, \tag{1.7}$$

where $A+B=L$. With this ''primitive'' breakup, Eq. (1.6) yields the second-order approximation for the short time propagator. The explicit form depends on the partitioning of the original Fokker–Planck operator $L=A+B$.[19–22] The neglect of the commutator of A and B often introduces a large error that has to be compensated by a small time step Δt, and consequently a large number N of steps in the path integral.

Here we suggest a simple alternative to the commonly used short time propagators, which admits much larger time steps in Eq. (1.5). It is based on a fourth-order symmetric factorization of the form

$$S_4(\Delta t)=e^{a\Delta tA}e^{\Delta tB/2}e^{\Delta tC}e^{\Delta tB/2}e^{a\Delta tA}, \tag{1.8}$$

with

$$C=(1-2a)A+\tfrac{1}{24}\Delta t^2\{2(1-6a+6a^2)[A,[B,A]]+(1-6a)[B,[B,A]]\}, \tag{1.9}$$

where a is an arbitrary number from the interval [0,1]. The above breakup is a straightforward generalization of the various decompositions available in the literature for the exponential operator. In particular, a known decomposition of De Raedt and De Raedt[24] follows from Eqs. (1.8) and (1.9) with $a=1/2$; while for $a=1/6$ and $a=(1-1/\sqrt{3})/2$ it reproduces two different factorizations recently derived by Suzuki[25] (see also Ref. 26). Although approximations like Eq. (1.8) are long-known[27] and have been frequently used for numerically solving many-body problems in classical mechanics, they have up to now rarely been applied to Fokker–Planck dynamics.[24,28] A reason for this seems to be the belief that the commutator appearing in Eq. (1.9) complicates the expression to such an extend that the calculation of P_4 is *always* impossible. Indeed, applying Eq. (1.8) to simple one-dimensional systems, one immediately runs into trouble, as it is unclear how to treat operators of the form $\exp\{\Delta t^3[f_3(x)\partial_{xxx}^3+f_2(x)\partial_{xx}^2+\cdots]\}$ containing higher than second order differential operators in the exponent, which arise in this case. For systems with more than one degree of freedom, the same complication arises if the diffusion matrix is invertible. However, for a system with a singular diffusion

matrix, the application of Eqs. (1.8) and (1.9) may result in a more accurate expression which is still as simple as the primitive Trotter splitting.

The above central observation is outlined in Sec. II for the example of the ordinary Brownian dynamics, Eq. (1.3), and for generalizations to memory friction and colored noise. Two numerical examples demonstrating the power of the new technique are presented in Sec. III. They include relaxation processes in a monostable system and in a double well. In the latter case, the transition rate is numerically calculated for two different temperatures and various different friction coefficients. In Sec. IV the numerical results are compared to different turnover theories now in use. Section V concludes the paper with final remarks.

II. FORMALISM

For convenience, we exclude the second commutator in Eq. (1.8) by setting $a=1/6$ so that

$$C=\tfrac{2}{3}A+\tfrac{1}{72}\Delta t^2[A,[B,A]]. \tag{2.1}$$

As a first simple example, we consider the one-dimensional Brownian motion in an external potential as defined by Eq. (1.3). In a second step, we shall indicate how the method can be adapted to arbitrary non-Markovian and multidimensional Brownian motion.

A. One-dimensional Markovian Brownian motion

We split the Fokker–Planck operator of Eq. (1.3) into one of a linear reference system,

$$B=-v\,\partial_x+\partial_v(rx+\gamma v)+\gamma D\partial_{vv}^2, \tag{2.2}$$

where r is an undetermined constant, and the rest

$$A=-G(x)\partial_v,\quad G(x)=rx-U'(x). \tag{2.3}$$

Insertion of Eqs. (2.2) and (2.3) into Eq. (1.7) yields the standard second-order approximation,[21]

$$P_2(x,v,\Delta t|x_0,v_0)=P_r[x,v-\tfrac{1}{2}\Delta tG(x),\Delta t|x_0,v_0+\tfrac{1}{2}\Delta tG(x_0)], \tag{2.4}$$

where $P_r(x,v,t|x_0,v_0)$ is the exact propagator of the linear reference system determined by Eq. (2.2). It is a Gaussian distribution which can be determined explicitly.[5] As a next step, we take into account higher-order corrections. To this end, we have to determine the operator C involved in Eq. (1.8). Using Eqs. (2.1), (2.2), and (2.3), we obtain

$$C=-Q(x)\partial_v,\quad Q(x)=\tfrac{2}{3}G(x)[1+\tfrac{1}{24}\Delta t^2G'(x)]. \tag{2.5}$$

Hence we find that the implementation of Eq. (1.8) is as simple as that of the Trotter formula, Eq. (1.7). The resulting fourth-order propagator reads

$$P_4(x,v,\Delta t|x_0,v_0)=\int dx_1dv_1P_r[x,v-\tfrac{1}{6}\Delta tG(x),\tfrac{1}{2}\Delta t|x_1,v_1+\Delta tQ(x_1)]\times P_r[x_1,v_1,\tfrac{1}{2}\Delta t|x_0,v_0+\tfrac{1}{6}\Delta tG(x_0)]. \tag{2.6}$$

Now it remains to determine the free parameter r so that the dynamics of the reference system resembles as closely as possible that of the full system. A simplest way for achieving this is to fix r by minimizing the anharmonic correction in a least-squares sense[21]

$$\partial_r\langle G^2(x)\rangle_s=0, \tag{2.7}$$

which immediately yields

$$r=\langle xU'(x)\rangle_s/\langle x^2\rangle_s. \tag{2.8}$$

Here $\langle\cdots\rangle_s$ means averaging over the equilibrium distribution

$$P_s(x)=Z^{-1}\exp[-U(x)/D]. \tag{2.9}$$

The variational approach to path integrals, which we have used here, is not new. It was first developed by Feynman in 1972.[29] In the last decade, Feynman's original technique has been considerably improved and extended.[30] The basic idea of the refined treatment is to define a harmonic reference system and to use its frequency as a variational parameter. This method can yield realistic finite temperature properties of quantum systems and also requires not much computer time. Only very recently, the variational path integral approach has been applied successfully to stochastic dynamics.[19,21,31]

B. Generalized Langevin equations

For many important applications in physics and chemistry, the Markovian assumption of white noise and instantaneous friction is not adequate. The Generalized Langevin equations (GLE) proposed by Zwanzig[6] allow a flexible description of the influence of an environment in thermal equilibrium that may have a long memory.

In the simplest one-dimensional case, the GLE has the form[6]

$$\dot{x}=v,\quad \dot{v}=-U'(x)-\int_0^t ds\,\gamma(t-s)v(s)+f(t), \tag{2.10}$$

where the Gaussian zero mean random force $f(t)$ is related to the friction kernel through the second fluctuation dissipation theorem

$$\langle f(t)f(s)\rangle=D\gamma(t-s). \tag{2.11}$$

The latter property ensures the equilibrium distribution of the standard Maxwell–Boltzmann form, Eq. (1.4). The memory friction must be a positive definite function, i.e., it must have a positive Fourier transform. In all other respects it may be an arbitrary function. Often an exponential form is assumed[9,18]

$$\gamma(t)=(\gamma/\tau)e^{-t/\tau}, \tag{2.12}$$

where τ is the correlation time of the noise, and γ the static friction

$$\gamma=\int_0^\infty ds\,\gamma(t). \tag{2.13}$$

In the limit $\tau\to 0$ the above correlation function reduces to the white noise delta function shown in Eq. (1.2) and the GLE (2.10) approaches the Markovian Langevin Eq. (1.1).

A standard trick to simplify the GLE with the exponential memory kernel is to introduce an additional variable,[12,13,18]

$$y=-\int_0^t ds\,\gamma(t-s)v(s)+f(t), \tag{2.14}$$

and rewrite the random force as

$$f(t)=\tau^{-1}\int_0^t ds e^{-(t-s)/\tau}F(s). \tag{2.15}$$

Now the new random force $F(t)$ is white, that is,

$$\langle F(t)F(s)\rangle=2\gamma D\,\delta(t-s), \tag{2.16}$$

thus resulting in a set of Markovian Langevin equations

$$\begin{aligned}\dot{x}&=v,\\ \dot{v}&=-U'(x)+y,\\ \tau\dot{y}&=-\gamma v-y+F(t).\end{aligned} \tag{2.17}$$

These equations are usually integrated numerically using the Verlet algorithm,[32] which is a straightforward analog of the Trotter formula (1.7).

In order to employ the above sketched idea of an improved short time propagator in the path integral, we proceed from the Langevin description, Eqs. (2.17), to the equivalent Fokker–Planck equation for the joint probability distribution of the three variables x, v, and y,

$$\begin{aligned}\partial_t P(x,v,y,t)=\{&-v\,\partial_x+[U'(x)-y]\partial_v+\tau^{-1}\partial_y(\gamma v+y)\\ &+\gamma\tau^{-2}D\partial_{yy}^2\}P(x,v,y,t).\end{aligned} \tag{2.18}$$

Then, splitting the operator of Eq. (2.18) into a linear Fokker–Planck operator of reference system

$$B=-v\,\partial_x+(rx-y)\partial_v+\tau^{-1}\partial_y(\gamma v+y)+\gamma\tau^{-2}D\partial_{yy}^2, \tag{2.19}$$

and an anharmonic correction given by Eq. (2.3), one finds that the operator C, Eq. (2.1), has exactly the same form as in the white noise limit, Eq. (2.5). This yields in a straightforward way

$$\begin{aligned}P_4(x,v,y,\Delta t|x_0,v_0,y_0)&\\ =\int dx_1dv_1dy_1P_r[x,v-\tfrac{1}{6}\Delta t G(x),y,\tfrac{1}{2}\Delta t|x_1,v_1&\\ +\Delta t Q(x_1),y_1]P_r[x_1,v_1,y_1,\tfrac{1}{2}\Delta t|x_0,v_0&\\ +\tfrac{1}{6}\Delta t G(x_0),y_0],&\end{aligned} \tag{2.20}$$

where $P_r(x,v,y,t|x_0,v_0,y_0)$ is the propagator of the linear reference system, which is now determined by Eq. (2.19). The stationary solution of Eq. (2.18) is known exactly

$$P_s(x,v,y)=Z^{-1}\,\exp\{-[U(x)+\tfrac{1}{2}v^2+\tfrac{1}{2}(\tau/\gamma)y^2]/D\}. \tag{2.21}$$

Integrating Eq. (2.21) over the noise variable y leads to the Maxwell–Boltzmann distribution as expected. Therefore, we can use Eq. (2.8) to fix the free parameter τ in this case as well.

C. Colored noise problem

In nonequilibrium (opened) systems, the friction can often be modeled by an instantaneous force, but finite correlations of the environment render the systems non-Markovian. Such processes are referred to as colored noise problems.[8,9,11,33] The simplest example is

$$\begin{aligned}&\dot{x}=v,\ \ \dot{v}=-\gamma v-U'(x)+f(t),\\ &\langle f(t)f(s)\rangle=(D/\tau)e^{-t/\tau}.\end{aligned} \tag{2.22}$$

Since the friction and the noise here are of different origin, the fluctuation dissipation theorem does not hold.

A Markov process, stochastically equivalent to Eqs. (2.22), can again be obtained by introducing an additional variable, $y=f(t)$, and rewriting the noise term in a similar way as in Eq. (2.15) to yield[33]

$$\begin{aligned}\dot{x}&=v,\\ \dot{v}&=-U'(x)-\gamma v+y,\\ \tau\dot{y}&=-y+F(t),\end{aligned} \tag{2.23}$$

where $F(t)$ is Gaussian white noise of strength D. The corresponding Fokker–Planck equation is

$$\begin{aligned}\partial_t P(x,v,y,t)=\{&-v\,\partial_x+\partial_v[U'(x)+\gamma v-y]+\tau^{-1}\partial_y y\\ &+\tau^{-2}D\partial_{yy}^2\}P(x,v,y,t).\end{aligned} \tag{2.24}$$

Splitting the operator of this equation into a linear contribution,

$$B=-v\,\partial_x+\partial_v(rx+\gamma v-y)+\tau^{-1}\partial_y y+\tau^{-2}D\partial_{yy}^2, \tag{2.25}$$

and the rest, Eq. (2.3), we again obtain for the operator C, Eq. (2.1), the same expression as in the white noise limit, Eq. (2.5). The resulting fourth-order approximation reads

$$\begin{aligned}P_4(x,v,y,\Delta t|x_0,v_0,y_0)&\\ =\int dx_1dv_1dy_1P_r[x,v-\tfrac{1}{6}\Delta t G(x),y,\tfrac{1}{2}\Delta t|x_1,v_1&\\ +\Delta t Q(x_1),y_1]P_r[x_1,v_1,y_1,\tfrac{1}{2}\Delta t|x_0,v_0&\\ +\tfrac{1}{6}\Delta t G(x_0),y_0],&\end{aligned} \tag{2.26}$$

where the reference propagator $P_r(x,v,y,t|x_0,v_0,y_0)$ is now determined by Eq. (2.25).

Before closing we recall that, unlike Eqs. (1.3) and (2.18), the Fokker–Planck equation for the colored noise problem, Eq. (2.24), does not obey detailed balance and therefore its stationary solution is not known exactly. In such a case, we suggest to employ in Eq. (2.8) the stationary distribution $P_r(x,v,y,t\to\infty)$ of the reference system instead of the unknown stationary solution P_s of the full nonlinear system. The resulting equation is easily solved for r by any root finding procedure. Generalizations of the method to cases with many degrees of freedom and non-Markovian processes with arbitrary memory kernels are given in Appendix A.

D. Numerical implementation

Comparing the short time approximations obtained in the present paper for the propagator of the Kramers model and its generalizations to time-dependent friction and colored noise (see also Appendix A) shows that they differ only by the particular forms of the reference propagators P_r used. The latter refer to linear systems and can be analytically evaluated for any number of degrees of freedom.[5] Substituting these short time approximations into Eq. (1.5), one obtains the high-accuracy discrete path integral representations we are looking for. Since the decomposition employed, Eq. (1.8), is symmetric in the sense that

$$S_4(-\Delta t)S_4(\Delta t)=1, \tag{2.27}$$

all these representations have an asymptotic error expansion, which contains only *even* powers of $1/N$. Therefore, extrapolation methods can be used to further improve the precision.[19,31,34] For example, an operator without the $1/N^4$ error is

$$S_6(t)=\tfrac{1}{15}[16S_4(t/2N)^{2N}-S_4(t/N)^N]. \tag{2.28}$$

Finally, we briefly discuss methods available for evaluating path integrals. Three general approaches are possible. The simplest iterative procedure involves multiplication of a propagator matrix times a vector representing a distribution function and therefore scales as M^2, where $M=\Pi_{i=1}^{m} M_i$ is the total number of grid points in the chosen discrete representation of the distribution function.[35] Here m is the number of degrees of freedom and M_i is the number of grid points in the ith degree of freedom. Because of the memory requirements and CPU constraints the utility of this procedure is limited to two-dimensional systems. Yet another grid-based approach utilizes fast Fourier transforms (FFT).[36] Although path integral representations of stochastic dynamics are, in general, not suitable for the FFT, a way to overcome this problem was developed in a previous paper.[31] The method employs the Stirling interpolation to dynamically readjust the distribution function at each time step with a mild increase in cost and with no loss of precision. The favorable scaling of the FFT, which is almost linear in the total number M of grid points, $M\ \log_2 M$, makes this approach much more efficient than matrix multiplication techniques. However, FFT algorithms require discretizations with M_i being a power of 2. In practice, often 64 grid points per variable are necessary for convergence. This limits the practical applicability of the method to systems with three dimensions at most. Finally, the multidimensional integral in Eq. (1.5) can be evaluated using global integration techniques. In the case of Brownian motion, an attractive feature of this approach is that the Gaussian integrals over velocities and additional (environmental) variables can be integrated out *analytically*, leaving us with a path integral for positions only. The effects of the environment enter via an influence functional. However, the latter is nonlocal in time, and therefore the resulting path integral cannot be evaluated by an iterative procedure. Shortly speaking, adopting the influence functional approach amounts to give up the Markovian property of the multidimensional distribution function for the sake of eliminating the velocity and environmental degrees of freedom. Thus Monte Carlo methods[37] are necessary in this case.

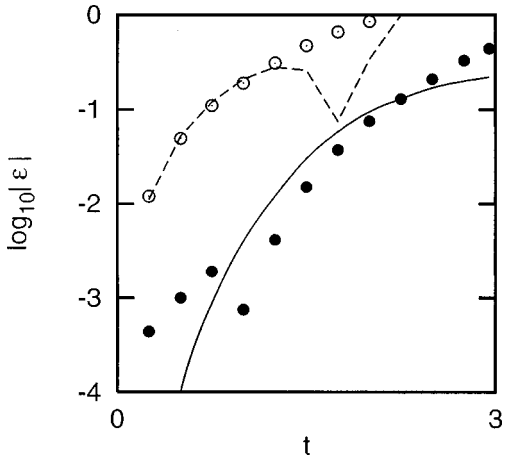

FIG. 1. Logarithm of the relative error, Eq. (3.2), in the second cumulants M_x and M_v for a linear Kramers model, Eqs. (1.3) and (3.1), calculated by means of the Trotter approximation (2.4) (open circles and dashed line) and the fourth-order propagator (2.6) (solid circles and solid line).

III. NUMERICAL RESULTS

For computational simplicity, we restrict our subsequent considerations to the conventional Kramers model given by Eq. (1.3). Moreover, we set from here on $D=1$. The method used to efficiently evaluate the quadrature in Eqs. (1.5) and (2.6) is described in a previous paper.[31] The aim of this section is twofold. First, we would like to illustrate the power of the present technique in yielding precise numerical results. This is done by calculating the propagator of the Fokker–Planck equation of a linear system, whose exact solution is known in advance. Our numerical test also includes a nonlinear model, for which only the stationary distribution is known exactly. Second, we present accurate calculations of activated rate processes in a symmetric double well. The transition rate, that is given by the least nonvanishing eigenvalue of Eq. (1.3), is numerically determined for two different barrier heights and various different friction coefficients.

A. Test calculations

Because closed-form analytic time dependent solutions are only available for the dynamics of a linear Fokker–Planck equation with

$$U(x)=\tfrac{1}{2}\alpha x^2, \tag{3.1}$$

we first tackle this problem to illustrate the power of the present technique. To make our test meaningful we set $r=0$, thus taking free Brownian as the reference system. Figure 1 shows the relative errors

$$\epsilon=[(\text{approximate})-(\text{exact})]/(\text{exact}) \tag{3.2}$$

of the second cumulants, $M_q=\langle q^2(t)\rangle-\langle q(t)\rangle^2$, $q=x,v$, that result when Eqs. (2.4) and (2.6) are used as *single step propagators*. As the initial distribution of position and velocity a δ-function is used, giving initially vanishing cumulants. The calculation is performed for $\gamma=\alpha=x_0=v_0=1$. As anticipated, the error made by the Trotter-approximated propa-

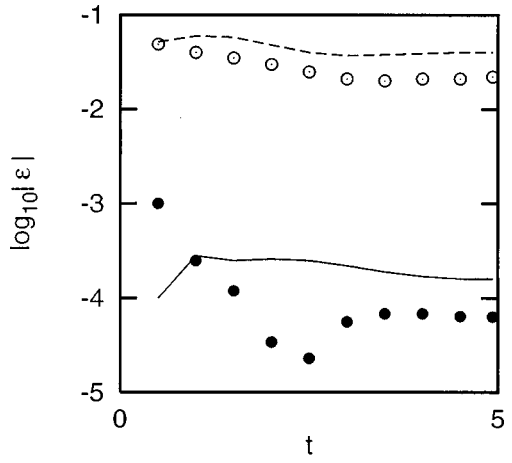

FIG. 2. Same as in Fig. 1 but for the path integral evaluation, with $\Delta t = 0.5$, of the same quantities.

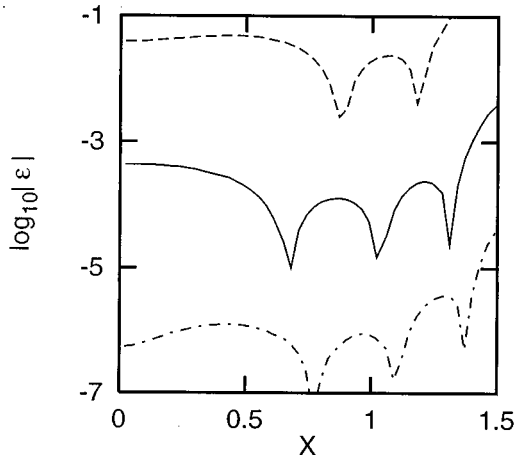

FIG. 3. Logarithm of the relative error due to the path integral evaluation, with $\Delta t = 0.1$, of the stationary solution $P_s(x)$, Eq. (2.9), for a double well, Eq. (3.5) with $E = 5$. The dashed and solid lines are for Eqs. (2.4) and (2.6), respectively. The dot–dashed line is for results after removal of quartic errors by means of Eq. (2.28).

gator, Eq. (2.4), rapidly increases with t, and very soon reaches 100%. In contrast, use of the present fourth-order propagator, Eq. (2.6), reduces the error over a broad range of t by nearly two orders of magnitude. This allows us to accurately calculate not only short, but also intermediate time dynamics.

However, the primary purpose of Eq. (2.6) is an improved short time propagator for the use in a path integral. Figure 2 shows the errors of the same quantities made by Eqs. (2.4) and (2.6) in the path integral evaluation according to Eq. (1.5). The bottom curve in the figure clearly illustrates that an accuracy of four significant digits is achieved by the fourth-order propagator with a discretization as coarse as $\Delta t = 0.5$. This feature of the present technique is particularly important when studying processes with noninvertible diffusion matrices like those governed by Eqs. (1.3), (2.18), and (2.24). In such a case, the second cumulant of the variable x as defined above, tends to zero as[23]

$$M_x = \tfrac{2}{3}\gamma\Delta t^3 + O(\Delta t^4), \tag{3.3}$$

rather than linearly

$$M_i = \Delta t D_{ii} + O(\Delta t^2), \tag{3.4}$$

as is the case for processes with invertible diffusion matrices. This means that with $\Delta t \to 0$ the short time propagator rapidly degenerates into a δ-function, requiring very fine spatial discretization. The latter substantially increases the storage requirements and execution time necessary to get good resolution for short time increments, which in turn are necessary for accuracy. In this context, it is difficult to overstate the usefulness of the method outlined in Sec. II. It leads to accurate results with relatively large time steps Δt and thus avoids using large dimensional matrices. For comparison, the error made by the Trotter-approximated propagator is by two orders of magnitude larger than that of the present short time propagator, and a precision of 10^{-4} is attainable in calculations with Eq. (2.4) only for $\Delta t \lesssim 0.05$.

B. Activated rate processes in a double well

As a second and more challenging example, we consider the Kramers model with a symmetric double well potential of the form

$$U(x) = E(x^2 - 1)^2, \tag{3.5}$$

where E is the height of the potential barrier in units of the thermal energy. Only the equilibrium distribution is known exactly in this case. In order to test the different path integral schemes, the equilibrium distribution was calculated for different values of E, γ, x_0, and v_0. Within the accuracy of calculations the results obtained turn out to be independent of γ and the initial conditions (x_0, v_0). Since the stationary distribution is symmetric, results for $E = 5$ are only shown for $x \geqslant 0$ in Fig. 3. The figure presents the relative errors of $P_s(x)$ that are caused by the path integral evaluation with $\Delta t = 0.1$, when using the various different short time propagators as discussed in Sec. II. As expected, the error attained with the fourth-order propagator, Eq. (2.6), is again much smaller than that obtained with the Trotter approximation, Eq. (2.4). It is also seen that the use of the extrapolation (2.28) further improves the accuracy of the present technique by nearly two orders of magnitude.

Finally, in Table I, we provide a list of the least nonvanishing eigenvalue λ_1 for $E = 5$ and 10 and for different values of γ. The calculations were performed with discretizations $\Delta t = 0.1$ and 0.05. The extrapolation formula (2.28) was then used to remove errors of order $1/N^4$. The least nonvanishing eigenvalue is extracted from the time evolution of the reactive flux

$$J(t) = \int_{-\infty}^{\infty} dv\, v P(0, v, t), \tag{3.6}$$

where $x = 0$ is the coordinate of the transition point. The reactive flux can always be written in the form

$$J(t) = \exp\left[- \int_0^t ds\, k(s) \right], \tag{3.7}$$

TABLE I. First nonzero eigenvalue λ_1 for the Kramers problem, Eqs. (1.3) and (3.5). Exponential notation $-k$ means that the number preceding is to be multiplied by 10^{-k}.

γ	$E=5$	$E=10$
200	0.2775-3	0.3914-5
100	0.5543-3	0.7807-5
30	0.1818-2	0.2513-4
20	0.2670-2	0.3610-4
10	0.4847-2	0.6078-4
8	0.5709-2	0.6929-4
6	0.6857-2	0.7973-4
4	0.8380-2	0.9250-4
3	0.9271-2	0.9977-4
2	0.1006-1	0.1069-3
1.5	0.1016-1	0.1092-3
1	0.9545-2	0.1066-3
0.75	0.8664-2	0.1004-3
0.5	0.7116-2	0.8684-4
0.25	0.4536-2	0.5933-4
0.1	0.2198-2	0.3041-4
0.05	0.1203-2	0.1717-4
0.01	0.2695-3	0.3992-5

where the function $k(t)$ determines the rate of the equilibration process. With increasing t, this function rapidly reaches a constant value, which coincides with the lowest nonzero eigenvalue of the Fokker–Planck Eq. (1.3).

In order to improve convergence, we started our calculations from the strong damping limit, $\gamma \gg \omega_0 = \sqrt{-U''(0)}$, where the Kramers trial function is known to be a good approximation to the true eigenfunction corresponding to λ_1. In this limit, the position of the particle completely describes the state of the system, and the process is governed by the following Smoluchowski equation,[2]

$$\gamma \partial_t P(x,t) = \partial_x [U'(x) + \partial_x] P(x,t). \tag{3.8}$$

The last equation can readily be solved by a standard basis set method to give the asymptotic solutions $(\gamma\lambda_1)_{\gamma\to\infty} = 0.055\,52$ and $0.000\,783\,5$ for $E=5$ and 10, respectively.[17] These asymptotic solutions agree well with the results obtained for $\gamma = 200$ in terms of the two-dimensional Fokker–Planck Eq. (1.3), $\gamma\lambda_1 = 0.055\,50$ and $0.000\,782\,8$, respectively.

We used the Kramers function to construct an appropriate initial distribution for the largest value of γ involved in the calculation. The distribution was propagated in time until $k(t)$ had reached a plateau value. The resulting final distribution was then used as initial distribution for the next smaller value of γ. Typical curves $k(t)$ extracted in this way from the time evolution of the reactive flux are displayed in Fig. 4 for $E=5$ and for $\gamma = 6$, 1.5, and 0.5.

The results shown in the table demonstrate the applicability of our methodology to practically all regimes of chemical interest, reaching from the extremely underdamped Brownian motion to the spatial diffusion regime. These results provide the necessary foundation for testing various different turnover theories that are already available in the literature. We emphasize that the present method is rather insensitive with respect to the choice of $U(x)$ and thus offers a universal tool for numerically treating the escape problem with a nonparabolic potential barrier for which no turnover theory exists.

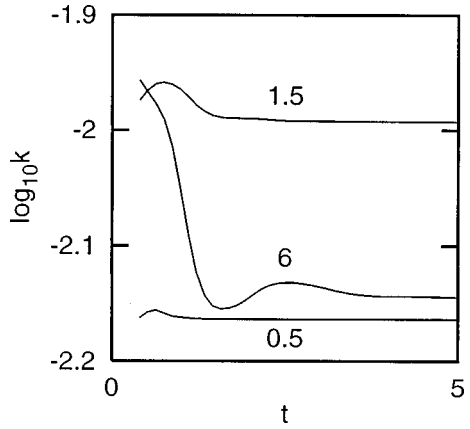

FIG. 4. Time evolution of the function $k(t)$ [Eq. (3.7)] for $E=5$ and $\gamma = 0.5$, 1.5, and 6.

IV. KRAMERS' THEORY OF THERMAL ACTIVATION

For a wide range of parameters, the equilibration process of a bistable system is determined by the transition rate from one well into the other. In a symmetric potential the least nonvanishing eigenvalue of the corresponding Fokker–Planck operator is then given by twice this rate[5]

$$\lambda_1 = \kappa \Gamma_{\mathrm{TST}}, \tag{4.1}$$

where Γ_{TST} is the transition state theory result

$$\Gamma_{\mathrm{TST}} = \frac{\omega_1}{\pi} e^{-E}, \quad \omega_1^2 = U''(1), \tag{4.2}$$

and κ is a transmission coefficient describing the deviation of the rate from Γ_{TST}. The problem of escape of a Brownian particle from a metastable state was first formulated by Kramers in his pioneering paper.[2] Kramers derived rate expressions valid in the limiting cases of weak and intermediate to strong friction and noticed the existence of a turnover region.

An asymptotic solution in the weak friction range was derived by Mel'nikov and Meshkov (MM).[38] A systematic solution of the full Kramers turnover problem was given by Grabert[39] and co-workers[40] (PGH) who generalized the theory to an arbitrary time-dependent friction, Eq. (2.10), and showed that the MM turnover formula can be obtained without any ad hoc bridging. These results are briefly reviewed in Appendix B. The key quantity appearing in both turnover theories is the energy loss of the particle per oscillation. The theories only differ in the determination of this quantity. In the weak damping limit, $\gamma \to 0$, the PGH energy loss, Eqs. (B4)–(B7), reduces to that of the MM theory, Eq. (B2), and may deviate considerably from the latter otherwise.

More recently in an effort to remove the large differences, which had been found in the underdamped regime, between analytical calculations and numerically exact results, Mel'nikov suggested a systematic approach to include

finite-barrier corrections to the escape rate.[41] However, the modified method though more accurate than the original MM theory appears to be rather complicated for practical applications. An alternative approach to this problem has also been put forward by Pollak and Talkner,[42] but its utility is restricted to the spatial diffusion regime.

Although it was shown that taking into account finite-barrier corrections improves the agreement with exact numerical results,[42,43] a detailed understanding of the range of validity of the above turnover theories is still lacking. In particular, it has remained unclear whether the large deviations between the MM theory and the true rate observed in the turnover region can mainly be attributed to finite-barrier effects. Yet another interesting question is whether the same deviations are also present in the PGH theory, as stated by Mel'nikov and co-workers.[43] Unfortunately the authors of Ref. 43 have not confirmed the validity of their statement by comparing the PGH theory with numerical results. The lack of answers to these questions is not surprising because almost all numerical investigations[18,22] are based on computer simulations schemes that are inappropriate for the present purpose. We mention just two reasons. First, in the weak friction limit, where the large deviations occur, simulations over long times are required. Second, in order to get a good statistics, one has to generate a huge number of trajectories. Otherwise statistical errors may be even larger than the difference between different turnover theories. Some of the above posed problems can be clarified by comparing both turnover theories with the numerical results for the least nonvanishing eigenvalue presented in Table I. But, before doing so, we would like to review an effective way to correct these theories without extraordinary computational effort.[44]

Improve turnover theory. To begin with we note that the above turnover theories are asymptotic not only in the barrier height, but also in the energy loss. Therefore, the deviations of the theories from numerical results may not only arise from finite-barrier effects, but also from an incorrect dependence of the energy loss δ on the friction coefficient. According to Eq. (B2), this quantity goes to infinity with increasing γ regardless of the barrier height. The same is true for the modified Mel'nikov theory, in which finite-barrier corrections are taken into account.[41] Also, the energy loss given by Eqs. (B4)–(B7) can only be approximate. It increases up to twice the barrier height and then slowly decrease with γ going to infinity until a limiting value (approximately $1.6E$) is approached. By definition, however, the energy loss cannot be larger than the barrier height.

The starting point of our approach to resolve this problem is the observation that for large potential barriers, $E \gg 1$, the stochastic dynamics governed by Eqs. (1.1) and (3.5) can be well approximated by the deterministic equations of motion. The latter becomes more evident, if one rescales the variables of Eqs. (1.1) and (3.5) by the barrier frequency as

$$t \to \omega_0 t, \quad v \to v/\omega_0, \quad \gamma \to \gamma/\omega_0 .$$

This rescaling renders the deterministic contribution independent of the barrier height and the noise term proportional to the inverse square root of the barrier height,

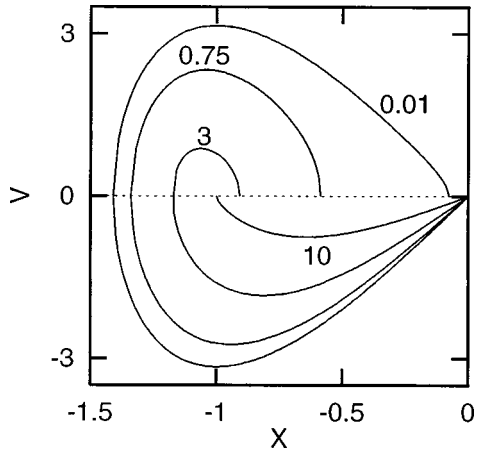

FIG. 5. Asymptotic deterministic trajectories [Eqs. (4.5)–(4.7)] for $E=5$ and $\gamma=0.01$, 0.75, 3, and 10.

$$\dot{x}=v, \quad \dot{v}=-\gamma v - x^3 + x + \sqrt{\gamma/(4E)}\,\xi(t), \tag{4.3}$$

where the Gaussian white noise $\xi(t)$ is normalized to

$$\langle \xi(t)\xi(0)\rangle = 2\,\delta(t). \tag{4.4}$$

Hence one may split the equations of motion into a leading contribution, describing the deterministic dynamics

$$\dot{x}=v, \quad \dot{v}=-\gamma v - U'(x), \tag{4.5}$$

and the fluctuating correction $\sqrt{\gamma/(4E)}\,\xi(t)$ and construct a perturbation expansion in powers of the inverse barrier height $1/E$. The latter may be considered as the formal smallness parameter.

In the present paper, we will not go beyond zero order in the perturbation. In this case, the energy loss is determined from the unperturbed (deterministic) equation of motion (4.5) for the asymptotic trajectory starting at the transition state, i.e., with energy E and period $T \to \infty$. Since no explicit solutions of Eq. (4.5) are known, it must be solved numerically with initial conditions

$$x(-T/2)=0, \quad v^2(-T/2) \ll 2E. \tag{4.6}$$

High efficiency is achieved by making use of the fourth-order factorization (1.8). A symplectic integration scheme based on this breakup is given in Appendix C. Typical asymptotic trajectories are shown in Fig. 5 for $E=5$. The energy loss is determined as the difference of the potential energy,

$$\delta = U(0) - U(x_2), \tag{4.7}$$

where x_2 is the point at which $v(t)$ crosses zero for the second time. With increasing damping coefficient, the value $|x_2|$ also increases, and beyond some γ ($\gamma \sim 10$) the particle reaches the bottom of the well without oscillations. The energy loss thus obtained is displayed in Fig. 6 as a function of the friction coefficient and compared with results of the MM and PGH theories. It is seen that for $\gamma \ll 1$ the deterministic energy loss reproduces the correct limiting formula (B2), while for $\gamma \gg 1$ it approaches the value $\delta = E$ as one expects. One finds that the PGH formula, Eqs. (B4)–(B8), gives a

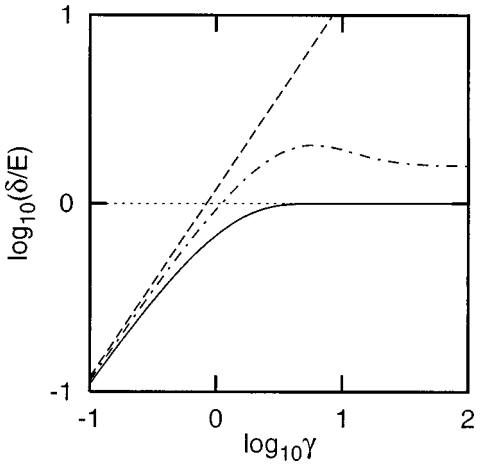

FIG. 6. Energy loss for a quartic potential, Eq. (3.5) with $E=5$, as a function of the friction coefficient. Dashed line, MM theory, Eq. (B2); dot–dashed line, PGH theory, Eqs. (B4)–(B8); solid line, deterministic approximation obtained in terms of Eqs. (4.5)–(4.7).

slightly larger energy loss. As we shall see, this provides a good agreement of the PGH theory with the exact numerical results in the spatial diffusion regime.

The relative errors made in the MM rate expression, Eq. (B1), by using two different approximations for the energy loss are displayed in Fig. 7 as functions of γ for two values of E. As anticipated, the use of the corrected energy loss in Eq. (B1) considerably improves the agreement of the MM theory with the exact numerical results. For small damping constants γ, the deviations of the errors of the MM theory for the different energy losses are rather small indicating that then the main source of the error is the finiteness of the barrier height as supposed by Mel'nikov in Ref. 41. The comparison of the errors for different barrier heights confirms this interpretation, see Fig. 7. However, as soon as the damping constant becomes larger than approximately 0.1, the asymptotic energy loss formula leads to an error comparable with, or even larger than the one caused by the finite barrier height.

Finally, the different turnover theories for the escape rate valid in the full damping range are compared in Fig. 8 with the exact numerical results for λ_1 given in Table I. As expected, in the weak damping regime the best agreement with the numerical results is achieved with the present definition of the energy loss, Eq. (4.5). Yet another interesting (perhaps surprising) finding is that the accuracy attained with the deterministic energy loss deteriorates with increasing γ rather than to further decrease as one might expect. A simple reason for this is that for $E=5$ the limiting value $\delta=E$ is not large enough to provide the equality $A(\delta)=1$, necessary for reducing Eq. (B3) to the right spatial diffusion limit. In contrast, the PGH theory, which predicts a larger energy loss, agrees well with the exact result in that case. On the other hand, with increasing E, the value $A(E)$ very rapidly reduces to unity and already for $E=10$ the deterministic energy loss provides a good agreement with the numerical results in the full damping range.

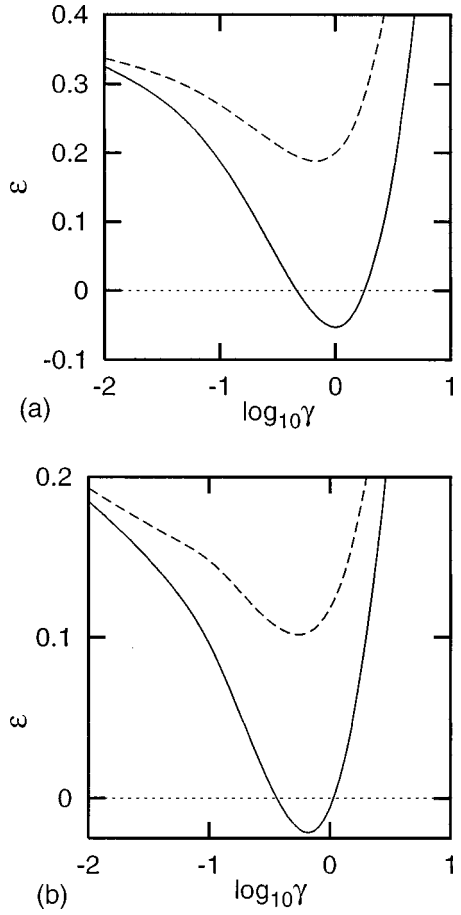

FIG. 7. Relative errors made in the MM rate formula, Eq. (B1), by using the MM approximation for the energy loss, Eq. (B2) (dashed line), and its correction obtained from the deterministic dynamics, Eqs. (4.5)–(4.7) (solid line). (a) $E=5$ and (b) $E=10$.

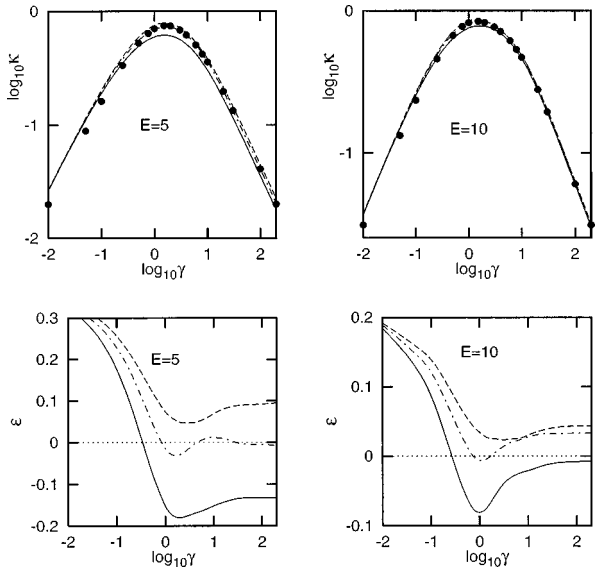

FIG. 8. Logarithm of the overall transmission coefficient, Eq. (B3), and relative errors made in κ by using different approximations for the energy loss. Dashed lines, MM theory, Eq. (B2); dot–dashed line, PGH theory, Eqs. (B4)–(B8); solid lines, deterministic energy loss, determined from Eqs. (4.5)–(4.7); circles, exact numerical results.

V. CONCLUDING REMARKS

In this paper, a rather fast, accurate, and easily applicable path integral method was developed for solving time-dependent Fokker–Planck equations with singular diffusion matrices. The power of the method is illustrated for a two-dimensional problem describing the motion of a Brownian particle in a potential field. The results obtained are very encouraging, since the time evolution of the propagator can quite accurately be evaluated in a wide range of the friction coefficient using rather large time steps Δt in a path integral. We have presented numerically exact results for rate constants of a classical symmetric double well system driven by noise and friction. These results allow us to analyze the escape problem without using ad hoc assumptions in a rather wide range of parameters, as well as to clarify the question of the validity of different turnover theories. We conclude that the existing theories are asymptotic not only in the barrier height, but also in the energy loss. We suggested an alternative rather simple way to evaluate this quantity, which improves the agreement between analytical and numerical results. A further improvement of the rate can be obtained by taking into account finite-barrier corrections.

Finally, we would like to emphasize that our presentation is not exhaustive with respect to methodology. Besides various different Fokker–Planck processes with singular diffusion matrices, the method outlined is also applicable to Hamiltonian systems, as well as to stochastic processes with invertible diffusion matrices in special cases where the Fokker–Planck operator obeys strict detailed balance.[45] As we already noted, the efficacy of the method can be substantially improved by using extrapolation techniques to remove the lower-order errors.[19,28,31] Yet another way to enhance its efficacy is to employ, instead of the Ornstein–Uhlenbeck process, an improved reference propagator that incorporates nonlinear aspects of the full system (see, e.g., Ref. 22). In all cases, our method permits a substantial reduction of the number N of time steps and thus substantially enlarges the time scales that can be covered by path integral calculations. In this way it extends the variety of problems that are computationally accessible.

APPENDIX A

The extension of Eq. (1.3) to the m-dimensional case, $\mathbf{x}=(x_1,\ldots,x_m)$, reads

$$\partial_t P(\mathbf{x},\mathbf{v},t)=\left\{-v_i\frac{\partial}{\partial x_i}+\frac{\partial}{\partial v_i}\left[\frac{\partial}{\partial x_i}U(\mathbf{x})+\gamma_{ij}\left(v_j+D\frac{\partial}{\partial v_j}\right)\right]\right\}P(\mathbf{x},\mathbf{v},t). \tag{A1}$$

Proceeding along the same line as in Sec. II, we obtain

$$P_4(\mathbf{x},\mathbf{v},\Delta t|\mathbf{x}^0,\mathbf{v}^0)=\int d\mathbf{x}^1 d\mathbf{v}^1 P_r[\mathbf{x},\mathbf{v}-\tfrac{1}{6}\Delta t\mathbf{G}(\mathbf{x}),\tfrac{1}{2}\Delta t|\mathbf{x}^1,\mathbf{v}^1+\Delta t\mathbf{Q}(\mathbf{x}^1)]P_r[\mathbf{x}^1,\mathbf{v}^1,\tfrac{1}{2}\Delta t|\mathbf{x}^0,\mathbf{v}^0+\tfrac{1}{6}\Delta t\mathbf{G}(\mathbf{x}^0)], \tag{A2}$$

where the vectors $\mathbf{G}$ and $\mathbf{Q}$ stand for

$$G_i(\mathbf{x})=r_{ij}x_j-\frac{\partial}{\partial x_i}U(\mathbf{x}),$$
$$Q_i(\mathbf{x},\Delta t)=\frac{2}{3}G_i(\mathbf{x})+\frac{1}{36}\Delta t^2 G_j(\mathbf{x})\frac{\partial}{\partial x_j}G_i(\mathbf{x}), \tag{A3}$$

and where the reference propagator $P_r(\mathbf{x},\mathbf{v},t|\mathbf{x}^0,\mathbf{v}^0)$ is defined by the linear operator

$$B=-v_i\frac{\partial}{\partial x_i}+\frac{\partial}{\partial v_i}\left[r_{ij}x_j+\gamma_{ij}\left(v_j+D\frac{\partial}{\partial v_j}\right)\right]. \tag{A4}$$

The elements of the matrix $\mathbf{r}$ involved in Eq. (A4) can also be determined by minimizing the anharmonic correction $\mathbf{G}$ to give

$$\mathbf{r}=\langle\mathbf{x}\cdot\nabla_x U(\mathbf{x})\rangle_s/\langle\mathbf{x}\cdot\mathbf{x}\rangle_s, \tag{A5}$$

where the average over x is performed with the distribution $P_s(\mathbf{x})=Z^{-1}\exp[-U(\mathbf{x})/D]$.

Finally, we outline the steps needed for a GLE, cf. Eq. (2.10), with an arbitrary memory friction $\gamma(t)$. To this end, we assume that the Laplace transform $\hat{\gamma}(z)$ has a continued fraction expansion, which can be approximated by its first m terms, as

$$\hat{\gamma}(z)=\int_0^\infty dt e^{-zt}\gamma(t)=\frac{\mu_1}{z+\gamma_1+}\frac{\mu_2}{z+\gamma_2+}\cdots\frac{\mu_m}{z+\gamma_m}. \tag{A6}$$

Here the parameters satisfy $\mu_i>0$, $\gamma_i\geqslant 0$. Then, introducing m auxiliary variables $\mathbf{y}=(y_1,\ldots,y_m)$, the one-dimensional non-Markovian process (2.10) is approximated by a m-dimensional Markov process.[13] Finally, this leads to

$$P_4(x,v,\mathbf{y},\Delta t|x_0,v_0,\mathbf{y}^0)=\int dx_1 dv_1 d\mathbf{y}^1 P_r[x,v-\tfrac{1}{6}\Delta t G(x),\mathbf{y},\tfrac{1}{2}\Delta t|x_1,v_1+\Delta t Q(x_1),\mathbf{y}^1]P_r[x_1,v_1,\mathbf{y}^1,\tfrac{1}{2}\Delta t|x_0,v_0+\tfrac{1}{6}\Delta t G(x_0),\mathbf{y}^0], \tag{A7}$$

where the functions G and Q are the same as for the white noise, Eqs. (2.3) and (2.5), while the reference propagator P_r is defined by

$$B=-v\frac{\partial}{\partial x}+\frac{\partial}{\partial v}(rx-y_1)+\frac{\partial}{\partial y_1}\left(\mu_1 v+\gamma_1 y_1-y_2+D\gamma_1\mu_1\frac{\partial}{\partial y_1}\right)+\frac{\partial}{\partial y_2}\left(\mu_2 y_1+\gamma_2 y_2-y_3+D\gamma_2\mu_1\mu_2\frac{\partial}{\partial y_2}\right)+\cdots+\frac{\partial}{\partial y_m}\left(\mu_m y_{m-1}+\gamma_m y_m+D\gamma_m\mu_1\cdots\mu_m\frac{\partial}{\partial y_m}\right). \tag{A8}$$

Since the noise in the GLE (2.10) obeys the fluctuation dissipation theorem, Eq. (2.11), the equilibrium distribution of

the non-Markovian internal noise process has the Maxwell–Boltzmann form (1.4), and the free parameter r can again be determined using Eq. (2.8).

APPENDIX B

To make the article self-contained we briefly outline in this appendix the central results of the MM and PGH turnover theories. Mel'nikov and Meshkov[38] showed that the transmission coefficient takes the form in the weak damping limit,

$$\kappa_{\mathrm{MM}}=A^2(\delta)/A(2\delta),$$
$$A(\delta)=\exp\left(\frac{1}{\pi}\int_0^\infty dx\,\frac{\ln\{1-\exp[-\delta(x^2+\frac{1}{4})]\}}{x^2+\frac{1}{4}}\right). \tag{B1}$$

Here δ is the dimensionless loss of energy per one oscillation of a particle with energy close to the barrier height. To lowest order in both the frictional damping and the inverse of the barrier height the energy loss is[38]

$$\delta=\gamma\int_{-T}^{T}dt\dot{x}^2(t)=2\gamma\int_0^{x_r}dx\sqrt{2[E-U(x)]}, \tag{B2}$$

with x_r being the turning point of the undamped trajectory, $U(x_r)=E$. In the MM theory, the overall transmission coefficient for the full damping range is given by the factor[38]

$$\kappa=(\mu/\omega_0)\kappa_{\mathrm{MM}},$$
$$\mu=\sqrt{\gamma^2/4+\omega_0^2}-\gamma/2. \tag{B3}$$

The factor μ assures that the bridging expression reduces to the correct spatial diffusion limit. For small ($\delta\ll 1$) and large ($\delta\gg 1$) values of the energy loss, the transmission coefficient (B3) reproduces the two limiting formulas of the Kramers theory.

The systematic solution of the Kramers turnover problem was given by Grabert[39] and co-workers[40] (PGH) who rederived Eq. (B3) without any ad hoc bridging and suggested a more correct (but also much more complicated) expression for the energy loss which reads

$$\delta=\frac{1}{2}\int_{-T}^{T}dt\int_{-T}^{T}dsK(t-s)F(t)F(s). \tag{B4}$$

In the last expression, the friction kernel $K(t)$ is determined by its Laplace transform

$$\hat{K}(z)=\frac{z}{a_0^2(z^2+\gamma z-\omega_0^2)}-\frac{z}{(z^2-\mu^2)}, \tag{B5}$$

with

$$a_0^2=\frac{2\mu}{2\mu+\gamma}, \tag{B6}$$

while the time-dependent force $F(t)$

$$F(t)=-a_0U_1'(a_0\rho) \tag{B7}$$

is determined from the zero-order equation of motion

$$\ddot{\rho}-\mu^2\rho=F(t), \tag{B8}$$

where $U_1(x)$ is a nonlinear part of the potential, $U_1(x)=U(x)+\omega_0^2x^2/2$. The asymptotic trajectory $\rho(t)$ starts at the barrier in the infinite past, traverses the well once, and returns to the barrier top at time $T\to\infty$.

APPENDIX C

The aim of this appendix is to outline a numerical scheme for efficiently integrating the deterministic equation of motion (B2). The solution to this equation can formally be written as

$$\begin{bmatrix}x(t+\Delta t)\\ v(t+\Delta t)\end{bmatrix}=e^{\Delta tL^+}\begin{bmatrix}x(t)\\ v(t)\end{bmatrix}, \tag{C1}$$

with the operator L^+ given by

$$L^+=v\,\partial_x-[U'(x)+\gamma v]\partial_v. \tag{C2}$$

Splitting L^+ into two parts, $L^+=A+B$ with

$$A=-U'(x)\partial_v,\quad B=v\,\partial_x-\gamma v\,\partial_v, \tag{C3}$$

and approximating the exponential operator $\exp(\Delta tL^+)$ by the fourth-order symmetric decomposition, Eqs. (1.8) and (2.1), we obtain the following symplectic integrator:

$$v_1=v_0-\tfrac{1}{6}\Delta tU'(x_0),\quad x_1=x_0+v_1(1-\alpha)/\gamma,$$
$$v_2=v_1\alpha-\Delta tQ(x_1),\quad x_2=x_1+v_2(1-\alpha)/\gamma, \tag{C4}$$
$$v_3=v_2-\tfrac{1}{6}\Delta tU'(x_2),$$

where $\alpha=\exp(-\gamma\Delta t/2)$, $x_0=x(t)$, $v_0=v(t)$, $x(t+\Delta t)=x_2$, $v(t+\Delta t)=v_3$, and where

$$Q(x)=\tfrac{2}{3}U'(x)[1-\tfrac{1}{24}\Delta t^2U''(x)]. \tag{C5}$$

Numerical applications show our method to be advantageous over standard finite-difference symplectic integrators now in use in that it provides very accurate results with rather large time steps for which the standard schemes break down.

[1] For recent reviews of the field, see B. J. Berne, M. Borkovec, and J. E. Straub, J. Phys. Chem. **92**, 3711 (1988); P. Hänggi, P. Talkner, and M. Borkovec, Rev. Mod. Phys. **62**, 251 (1990); V. I. Mel'nikov, Phys. Rep. **209**, 1 (1991); *Activated Barrier Crossing*, edited by P. Hänggi and G. Fleming (World Scientific, Singapore, 1992); *New Trends in Kramers' Reaction Rate Theory*, edited by P. Talkner and P. Hänggi (Kluwer Academic, Dordrecht, 1995).

[2] H. Kramers, Physica (Amsterdam) **7**, 284 (1940).

[3] S. Chandrasekhar, Rev. Mod. Phys. **15**, 1 (1943).

[4] C. W. Gardiner, *Handbook of Stochastic Methods* (Springer, Berlin, 1983).

[5] H. Risken, *The Fokker-Planck Equation, Methods of Solution and Applications*, 2nd ed. (Springer, New York, 1989).

[6] R. Zwanzig, J. Stat. Phys. **9**, 215 (1973).

[7] H. Mori, Prog. Theor. Phys. **53**, 1617 (1975); N. G. van Kampen, *Stochastic Processes in Physics and Chemistry* (Elsevier, Amsterdam, 1992), p. 233.

[8] For recent reviews, see *Noise in Nonlinear Dynamical Systems*, edited by F. Moss and P. V. E. McClintock (Cambridge University Press, Cambridge, 1989); K. Lindenberg and B. J. West, *The Nonequilibrium Statistical Mechanics of Open and Closed Systems* (VCH, New York, 1990); P. Jung, Phys. Rep. **234**, 175 (1993); P. Hänggi and P. Jung, Adv. Chem. Phys. **89**, 239 (1995).

[9] J. Stat. Phys. **55**, No. 5/6 (1989), special issue on external noise problems, edited by C. R. Doering, H. R. Brand, and R. E. Ecke.

[10] P. Grigolini, J. Chem. Phys. **89**, 4300 (1988); P. M. Rodger and M. G. Sceats, *ibid.* **92**, 2526 (1990).

[11] T. Fonseca and P. Grigolini, Phys. Rev. A **33**, 1122 (1986); P. Hänggi and

P. Jung, *ibid.* **35**, 4464 (1987); L. Schimansky-Geier, Z. Phys. B **79**, 451 (1990).
[12] D. R. Cox and H. D. Miller, *The Theory of Stochastic Processes* (Chapman and Hall, London, 1972), p. 262.
[13] E. Guardia, F. Marchesoni, and M. San Miguel, Phys. Lett. **100A**, 15 (1984).
[14] A. N. Drozdov, J. Chem. Phys. **105**, 515 (1996); Phys. Rev. E **55**, 1496 (1997).
[15] R. Lovett, J. Chem. Phys. **84**, 4602 (1986); B. Cartling, *ibid.* **87**, 2638 (1987); A. N. Drozdov and M. Morillo, Phys. Rev. E **54**, 931 (1996).
[16] P. B. Visscher, Phys. Rev. B **14**, 347 (1976); K. Voigtlaender and H. Risken, J. Stat. Phys. **40**, 397 (1985); **41**, 825 (1985); F. Marchesoni, Phys. Rev. B **32**, 1827 (1985); G. J. Moro and A. Polimeno, Chem. Phys. **131**, 281 (1989).
[17] A. N. Drozdov and P. Talkner, J. Chem. Phys. **105**, 4117 (1996).
[18] J. E. Straub, M. Borkovec, and B. J. Berne, J. Chem. Phys. **83**, 3172 (1985); **84**, 1788 (1986); P. Hänggi, T. J. Mroczkowski, F. Moss, and P. V. E. McClintock, Phys. Rev. A **32**, 695 (1985); S. C. Tucker, M. E. Tuckerman, B. J. Berne, and E. Pollak, J. Chem. Phys. **95**, 5809 (1991); J. B. Straus and G. A. Voth, *ibid.* **96**, 5460 (1992); G. K. Schenter, R. P. McRae, and B. C. Garrett, *ibid.* **97**, 9116 (1992); S. Linkwitz, H. Grabert, E. Turlot, D. Esteve, and M. H. Devoret, Phys. Rev. A **45**, 3369 (1992); M. M. Wu, K. Y. R. Billah, and M. Shinozuka, Phys. Rev. E **52**, 3377 (1995); J. S. Bader and B. J. Berne, J. Chem. Phys. **102**, 7953 (1995); A. Starobinets, I. Rips, and E. Pollak, *ibid.* **104**, 6547 (1996).
[19] For a recent review, see A. N. Drozdov and J. J. Brey, Phys. Rev. E **57**, 146 (1998).
[20] B. Carmeli, V. Mujica, and A. Nitzan, Ber. Bunsenges. Phys. Chem. **95**, 319 (1991); A. N. Drozdov, Phys. Lett. A **171**, 175 (1992).
[21] A. N. Drozdov, Physica A **196**, 258 (1993).
[22] M. Topaler and N. Makri, J. Chem. Phys. **101**, 7500 (1994).
[23] A. N. Drozdov and M. Morillo, Phys. Rev. Lett. **77**, 5324 (1996); A. N. Drozdov, Phys. Rev. E **55**, 2496 (1997).
[24] H. De Raedt and B. De Raedt, Phys. Rev. A **28**, 3575 (1983).
[25] M. Suzuki, in *Computer Simulation Studies in Condensed Matter Physics VIII*, edited by D. P. Landau, K. K. Mon, and H.-B. Schüttler (Springer, Berlin, 1996).
[26] S. A. Chin, Phys. Lett. A **226**, 344 (1997).
[27] For a review, see R. M. Wilcox, J. Math. Phys. **8**, 962 (1967).
[28] A. N. Drozdov and J. J. Brey, Phys. Rev. E **57**, 1284 (1998).
[29] R. P. Feynman, *Statistical Mechanics* (Benjamin, Reading, 1972).
[30] R. Giachetti and V. Tognetti, Phys. Rev. Lett. **55**, 912 (1986); R. P. Feynman and H. Kleinert, Phys. Rev. A **34**, 5080 (1986); P. Zhang, R. M. Levi, and R. A. Friesner, Chem. Phys. Lett. **144**, 236 (1988); G. A. Voth, D. Chandler, and W. H. Miller, J. Chem. Phys. **91**, 7749 (1989); C. H. Mak and H. C. Andersen, *ibid.* **92**, 2953 (1990); J. Cao and B. J. Berne, *ibid.* **92**, 7531 (1990); M. Messina, B. C. Garrett, and K. Schenter, *ibid.* **100**, 6570 (1994).
[31] A. N. Drozdov, J. Chem. Phys. **107**, 3505 (1997).
[32] M. P. Allen and D. J. Tildesley, *Computer Simulations of Liquids* (Oxford University Press, Oxford, 1987).
[33] M. M. Klosek-Dygas, B. J. Matkowsky, and Z. Schuss, Phys. Lett. A **130**, 11 (1988); F. Marchesoni, *ibid.* **130**, 467 (1988); T. J. Newman, A. J. Bray, and A. J. McKane, J. Stat. Phys. **59**, 357 (1990); V. E. Shapiro, Phys. Rev. E **48**, 109 (1993); S. J. B. Einchcomb and A. J. McKane, Physica A **216**, 128 (1995).
[34] K. E. Schmidt and M. A. Lee, Phys. Rev. E **51**, 5495 (1995).
[35] A. N. Drozdov and V. Yu. Zitserman, Phys. Lett. **94A**, 17 (1983); D. Thirumalai, E. J. Bruskin, and B. J. Berne, J. Chem. Phys. **79**, 5063 (1983); M. F. Wehner and W. G. Wolfer, Phys. Rev. A **27**, 2663 (1983); **28**, 3003 (1983); L. Ingber, Phys. Rev. E **49**, 4652 (1994); L. Ingber and P. L. Nunez, *ibid.* **51**, 5074 (1995).
[36] M. D. Feit, J. A. Fleck, Jr., and A. Steiger, J. Comput. Phys. **47**, 412 (1982); D. Koslof and R. Kosloff, *ibid.* **52**, 35 (1983).
[37] K. Binder and D. W. Heermann, *Monte Carlo Simulation in Statistical Physics* (Springer, Berlin, 1988).
[38] V. I. Mel'nikov and S. V. Meshkov, J. Chem. Phys. **85**, 1018 (1986).
[39] H. Grabert, Phys. Rev. Lett. **61**, 1683 (1988).
[40] E. Pollak, H. Grabert, and P. Hänggi, J. Chem. Phys. **91**, 4073 (1989).
[41] V. I. Mel'nikov, Phys. Rev. E **48**, 3271 (1993).
[42] P. Talkner and E. Pollak, Phys. Rev. E **47**, 21 (1993); E. Pollak and P. Talkner, *ibid.* **47**, 922 (1993); P. Talkner, Chem. Phys. **180**, 199 (1994).
[43] R. Ferrando, R. Spadacini, and G. E. Tommei, Phys. Rev. E **51**, 1645 (1995).
[44] A. N. Drozdov and J. J. Brey, Chem. Phys. (to be published).
[45] A. N. Drozdov, J. Chem. Phys. **108**, 6580 (1998).